

## Thermalization of Positronium in Gases

M. Skalsey, J. J. Engbrecht, R. K. Bithell, R. S. Vallery, and D. W. Gidley

*Randall Laboratory of Physics, University of Michigan, Ann Arbor, Michigan 48109*

(Received 17 October 1997)

The thermalization of positronium (Ps) formed at a few eV in gases is investigated using time-resolved, Doppler broadening measurements of the annihilation photons. Magnetic quenching permits energy measurements about 40 ns after Ps is formed in H<sub>2</sub>, N<sub>2</sub>, He, Ne, Ar, isobutane, and neopentane. The thermalization rate is measured by changing the gas density, and a classical elastic scattering cross section and a Ps formation energy are determined. The impact of Ps thermalization on decay rate experiments using gases is also discussed. [S0031-9007(98)05946-8]

PACS numbers: 36.10.Dr, 34.50.Bw, 78.70.Bj

Collisions between normal gas atoms and the exotic atom positronium (Ps, positron-electron bound state) are interesting and unique because Ps is so light relative to its target. Hence Ps, formed at typically a few eV in most gases, will thermalize very slowly if elastic scattering is the only available energy loss mechanism. In the elastic case, the fractional energy loss per collision is only of order  $m/M \sim 10^{-4}$  ( $m$  is the Ps mass,  $M$  is the atomic/molecular mass.) The low energy Ps-atom collision is also inherently quantum mechanical in nature since the de Broglie wavelength of Ps below 1 eV is greater than 9 Å, larger than the classical geometric atomic size. Moreover, it was recognized early [1] that cross section calculations must include the polarization/Van der Waals interaction and electron exchange. These features apparently complicate the calculations of cross sections, done presently including the exchange interaction for only one- and two-electron systems scattering Ps (H: [2]; H<sub>2</sub>: [3]; He: [4–9]). For example, the calculations for Ps-He elastic cross sections differ by as much as a factor of 5 while the H<sub>2</sub> calculation will be seen to be at least a factor of 10 above experimental results. Our present results will underscore the need for improved cross section calculations. Improvements in understanding the fundamental Ps-atom interaction will, in turn, through knowledge of scattering lengths, improve the understanding of Ps interactions with surfaces of condensed media.

Positronium as a scattering probe offers a unique experimental advantage since its annihilation into two photons provides a mechanism for determining its velocity and hence the rate of thermalization and the momentum transfer cross section ( $\sigma_m$ ) for gas targets. Previous measurements of Ps thermalization in gases [10–12] have all used the technique of angular correlation of annihilation radiation (ACAR) in which the small deviation from colinearity of two 511 keV photons is a measure of the *transverse* Ps momentum. Such ACAR measurements in pure gases are difficult because the low  $\beta$ -decay positron stopping power of the gases spreads out the Ps source so as to degrade the resolution to low energy Ps [10]. A second approach is to use silica (SiO<sub>2</sub>) aerogel filled with the target gas to produce a compact source of Ps [11]. This

procedure suffers from the systematic complication of deconvolving the effect of the Ps-aerogel collisions [11,12]. Furthermore, these ACAR techniques are not time resolved in that they do not distinguish the age of the Ps when it annihilates.

In this Letter, we report the measurement of Ps thermalization rates, formation energies, and momentum transfer cross sections in purely gaseous target using time-resolved Doppler Broadening Spectroscopy (DBS). In this complementary technique to ACAR, the Doppler broadening of the back-to-back annihilation photons observed in a single high-resolution Ge detector is a measure of the *longitudinal* momentum of the annihilating Ps. Timing information as well as DBS is derived from the Ge detector signal, enabling the direct correlation between age and energy of the Ps to be determined. The rate of thermalization and the average formation energy of Ps can then be determined. The gases used in this investigation include He, H<sub>2</sub>, and Ar for comparison to the theoretical calculations [3–7] and/or experimental results [12]. Also included are all of the gases used in a recent, precision orthopositronium (o-Ps) decay rate measurement [13]: Ne, N<sub>2</sub>, isobutane (C<sub>4</sub>H<sub>10</sub>), and neopentane (C<sub>5</sub>H<sub>12</sub>). The thermalization of Ps in these gases is an important systematic concern [13] to ensure that the collisional annihilation rate is constant throughout the time interval when the decay rate is measured.

The thermalization rate of Ps in a noble gas was calculated 30 years ago by Sauder [14], under the assumption of classical elastic scattering, i.e., an energy-independent cross section for energy loss (momentum transfer)  $\sigma_m$  which was interpreted as the classical geometrical atomic cross section. If Ps is formed at only a few eV, below the 5.1 eV threshold for excitation of the Ps or the noble gas (>10 eV) and slow enough to avoid collisional dissociation, Sauder's elastic model may be appropriate. The Ps kinetic energy  $E(t)$ , as it asymptotically approaches thermal energy,  $E_{th}$ , is given by [11,14]

$$E/E_{th} = \coth^2(\beta + \Gamma nt), \quad (1)$$

where  $\beta$  is related to the average initial energy  $E_0$  of Ps that can eventually thermalize:  $\coth^2 \beta = E_0/E_{th}$ .  $\Gamma$  is

the rate of thermalization normalized to the gas number density ( $n$ ). The value of  $\sigma_m$  is related to  $\Gamma$  from [14]

$$\Gamma = \frac{mM}{(m+M)^2} \sigma_m \sqrt{\frac{2E_{th}}{m}} \approx \frac{\sigma_m}{M} p_{th}, \quad (2)$$

where  $p_{th}$  is the momentum of thermalized Ps. Even when  $\beta \approx 0$  ( $E_0 \rightarrow \infty$ ), Ps approaches thermal equilibrium with a characteristic time  $\tau = (\Gamma n)^{-1}$ , such that after times of  $\tau$ ,  $2\tau$ , and  $3\tau$ , Ps has slowed to within 70%, 8%, and 1%, respectively, of  $E_{th}$ .

Measuring o-Ps thermalization with time-resolved DBS of the 511 keV photons was first done by Chang *et al.* [15] with o-Ps in evacuated SiO<sub>2</sub> aerogel. In this technique, a magnetic field ( $B_0 = 2.85$  kG in our apparatus) perturbs and admixes the two  $m = 0$  Ps states. The field-perturbed o-Ps state has a vacuum lifetime of 52 ns at  $B_0$  compared to 142 ns for the two unperturbed  $m = \pm 1$  o-Ps states. The perturbed o-Ps state also decays 64% of the time by  $2\gamma$ , yielding the 511 keV photons required for the DBS measurements. A high-resolution Ge detector observes the energy spectrum of the 511 keV photons from o-Ps formed and decaying in gases. The apparatus is essentially the same as [13] (see Fig. 1 therein) with the Ge detector situated above the gas chamber. A delayed time window, 30–50 ns after prompt events (parapositronium and direct  $e^+e^-$  annihilation), selects o-Ps events for energy analysis; the Ge detector has two outputs, one used for timing and the other for energy spectroscopy. The intrinsic resolution of the Ge detector (FWHM = 1.20 keV) is calibrated using the 511.86 keV nuclear  $\gamma$  ray obtained from a <sup>106</sup>Ru source.

The spectrum containing the 511 keV o-Ps peak is modeled as the sum of two Gaussians with the same centroid and a step function (at 511 keV) in the background. These shapes are then convolved with the intrinsic resolution obtained from the <sup>106</sup>Ru source. A region of  $\pm 19$  keV surrounding the 511 keV peak is fit with the resolution-convoluted, two-Gaussian shape, as shown in Fig. 1. The Doppler broadening of the o-Ps is measured by the narrower of the two Gaussians. The wider Gaussian contains a number of components involving  $e^+$  annihilation with higher momentum molecular electrons, including (1) annihilation of o-Ps colliding with gas molecules; (2) direct annihilation of slow  $e^+$ , i.e.,  $e^+$  that have lost too much energy to form Ps; and (3) uncorrelated, random background in the delayed time window. The  $3\gamma$  o-Ps continuum spectrum, which cuts off at 511 keV, and small-angle Compton scattering of 511 keV photons lead to the step function in the background. The background is fit to two straight lines with slopes on either side of the step. A small fraction of o-Ps  $3\gamma$  continuum decays will have two photons emitted in almost the same direction, so that both simultaneously strike the Ge detector. This  $2\gamma$  effect leads to a tail on the high energy side of the 511 keV peak [16]. A 1.6-mm-thick Pb shield is placed between the detector and the Ps source in order to reduce this  $2\gamma$  tail to a negligible amplitude as shown in Fig. 1.

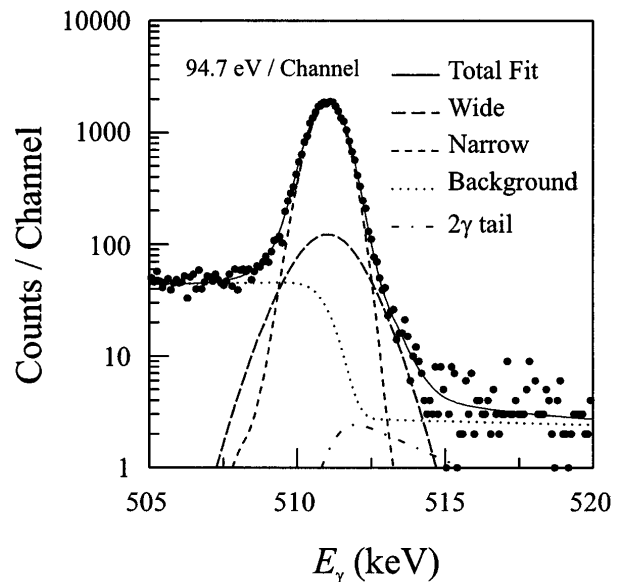


FIG. 1. Typical thermalization data. The Doppler broadened 511 keV photopeak is resolved into two Gaussians, a step background, and a  $2\gamma$  tail. The first three components are shown convoluted with the intrinsic detector resolution; the  $2\gamma$  tail is also convoluted with the narrow Gaussian.

The direct annihilation of  $e^+$  is not well described by a single Gaussian [17] due to annihilation with high momentum core electrons. Therefore, if the relative fraction of slow  $e^+$  annihilation becomes too large, the fit obtained for the narrow component becomes speciously broadened. To minimize this effect we have utilized a variety of functional forms to fit the wide component, with the most successful being a “modified” Gaussian (the Gaussian exponent of 2.0 is replaced with an empirically determined value of 1.64). Then, if the narrow component fitting with modified and Gaussian wide components is not consistent, it is excluded from the final results. Data not used for this reason are low pressure isobutane and neopentane and higher pressures of H<sub>2</sub>, He, Ne, Ar, and N<sub>2</sub>. Two systematic errors are included in the results to account for residual model dependence and resolution variations. For Ne and Ar, the model dependence systematic is the largest contributor to the final error in the thermalization rate. The intrinsic resolution of the Ge detector also limits the minimum narrow Gaussian width reliably fitted to 40% of the intrinsic Ge width.

The fitted result for the width of the narrow Gaussian (FWHM:  $W_{Ps}$  in keV) is used to calculate a rms average energy of o-Ps ( $E$  in eV) from [18]

$$E(\text{eV}) = [1.0288W_{Ps}(\text{keV})]^2. \quad (3)$$

In deriving this Doppler broadening formula, it is only assumed that the thermalizing Ps has a Maxwell-Boltzmann distribution of isotropic velocities which then yields a Gaussian in the DBS spectrum. There is no evidence from this investigation that the narrow Ps component is not a Gaussian, but sensitivity to this feature is not high.

Using this method,  $E$  is determined after various numbers of gas collisions by changing the density of the gas while keeping the delayed time window fixed at 30–50 ns. It is important to note that this observation of thermalization is model independent, in contrast to the previous ACAR studies [10–12]. The values of  $E$  vs  $nt$  can then be related to the classical elastic thermalization model by inverting Eq. (1) to yield  $\text{arccoth}\sqrt{E/E_{\text{th}}} = \Gamma nt + \beta$ . In Fig. 2, we plot  $\text{arccoth}\sqrt{E/E_{\text{th}}}$  vs  $n\bar{t}$ , where  $\bar{t} = 38$  ns is the weighted average of the delayed time window and  $n$  is expressed in amagats, the density unit corresponding to one atmosphere pressure at STP for which  $n = 2.69 \times 10^{19}/\text{cm}^3$ . The slope of the lines in Fig. 2 is therefore  $\Gamma$ , the thermalization rate at one amagat, and the intercept  $\beta$  determines the average initial energy  $E_0$ . Results for  $\Gamma$  and  $E_0$  are found in Table I.

As can be seen in Fig. 2, a clear advantage of this  $nt$ -resolved DBS technique over the ACAR methods is that one can test the validity of the elastic thermalization model by observing the linearity of the data. The good, linear fits of the noble gas data are not surprising, given our limited sampling range of o-Ps energies. However, for polyatomic gases where *inelastic* scattering dominates, the curve should roll over at high  $nt$  as some of the internal degrees of freedom become less accessible at low  $E$ . The fitted slopes should therefore be considered an “effective  $\Gamma$ ” for this particular o-Ps energy range. In addition, as  $nt \rightarrow 0$  all of the data approach nearly common intercepts corresponding to average initial energies  $E_0$  in the range of 2–4 eV. This is completely consistent with the expectation that Ps with  $E > 6.8$  eV (the Ps binding energy) will likely dissociate before thermalizing, and hence values of  $E_0 \approx 6.8/2$  eV are reasonable.

The slopes of the data in Fig. 2 and the corresponding fitted values of  $\Gamma$  in Table I, and hence  $\sigma_m/M$ , vary by

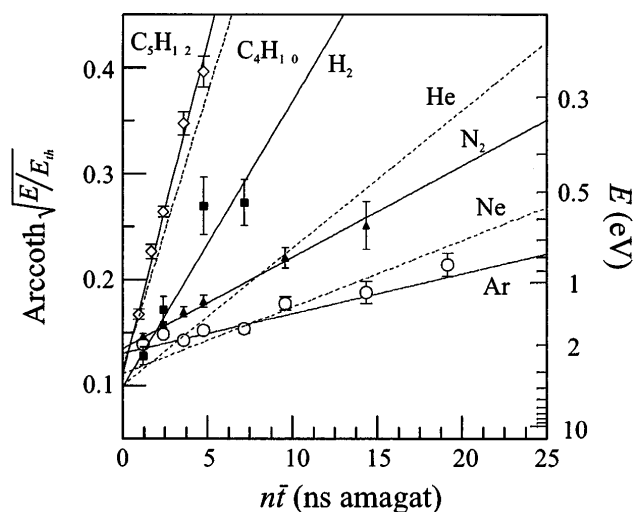


FIG. 2. Fits to Sauder’s thermalization model [13]. The slope of each line gives the Ps thermalization rate for the indicated gases. The zero intercepts are the average initial energies. Only the fitted lines are shown for isobutane, He and Ne. These data are omitted for clarity.

nearly a factor of 20 and apparently order by the mass of the *atom* struck, along with some *molecular* size factor. Specifically, the  $\text{N}_2$  data fall between He and Ne with  $M$  values of 4 and 20, respectively, consistent with the atomic mass of 14 for N. The  $\text{H}_2$  and hydrocarbons, for which we assume H is the struck atom, all thermalize Ps faster than He and order by molecular size (i.e., number of H atoms). Clearly, the molecular masses of isobutane and neopentane, 58 and 72, respectively, are not explicitly relevant. Such trends can be qualitatively understood from the fact that Ps, even thermalized, is so fast that collision times permit only the struck atom to recoil, not the whole molecule. These intuitive results are quite different from those in Ref. [11] in which the thermalization rate determined by ACAR is claimed to be equal for He [12], Ne, and isobutane.

Unfortunately, quantitative comparison with previous ACAR measurements is difficult because the results in Ref. [10] are not absolute, but relative, measurements (and hence no errors are quoted), and the results in Ref. [11] are subject to a systematic error in the treatment of the aerogel thermalization effect and values of  $\sigma_m$  for He,  $\text{H}_2$ , and Ar have subsequently been revised downward by factors of 3–5. The revised values [12] to be compared with those in Table I are now (in units of  $10^{-16} \text{ cm}^2$ )  $\sigma_m(\text{He}) = 11 \pm 3$ ,  $\sigma_m(\text{H}_2) = 17 \pm 5$ , and  $\sigma_m(\text{Ar}) = 15 \pm 10$ . Although these cross sections are for a Ps energy of  $E \sim 0.3$  eV, somewhat lower than our average  $E$  of about 1 eV, the agreement for He and  $\text{H}_2$  is still not good. The theoretical and experimental results for these two gases are summarized in Fig. 3. The calculation of  $\sigma_m(\text{H}_2)$  [3] is probably too high, having neglected polarization effects. There is also a wide spread in the He calculations, especially considering recent unpublished results [8,9] which are significantly lower than the published values and in agreement with the present measurement. Our He value may be consistent with the scattering length measurement [19] and calculation [6] (the zero energy cross sections in Fig. 3) if the energy

TABLE I. Results of Ps thermalization measurements in gases. The table displays  $1/\Gamma$ , the inverse of the Ps thermalization rate per amagat (am.), i.e., at one atmospheric pressure (STP); the average formation energy for Ps,  $E_0$ ; the energy interval of the measurements,  $\Delta E$ ; the derived elastic scattering cross section for momentum transfer,  $\sigma_m$ . For molecular gases, it is assumed that  $M$  in Eq. (2) is that of the molecule.

Gas	$1/\Gamma$ (ns $\times$ am.)	$E_0$ (eV)	$\Delta E$ (eV)	$\sigma_m$ ( $\text{\AA}^2$ )
$\text{H}_2$	$35 \pm 6$	$3.9^{+0.9}_{-0.7}$	0.54–2.35	$2.4 \pm 0.4$
He	$72 \pm 11$	$4.0^{+1.5}_{-1.0}$	0.38–1.45	$2.3 \pm 0.4$
Ne	$147 \pm 22$	$3.1^{+0.4}_{-0.3}$	0.38–1.93	$5.7 \pm 0.8$
Ar	$257 \pm 50$	$2.22^{+0.09}_{-0.09}$	0.88–2.05	$6.5 \pm 1.3$
$\text{N}_2$	$115 \pm 12$	$2.06^{+0.10}_{-0.09}$	0.48–1.85	$10.2 \pm 1.1$
$\text{C}_4\text{H}_{10}$	$17 \pm 2$	$3.4^{+2.1}_{-1.1}$	0.31–0.80	$144 \pm 19$
$\text{C}_5\text{H}_{12}$	$14 \pm 1.2$	$3.3^{+0.7}_{-0.5}$	0.27–1.42	$208 \pm 17$

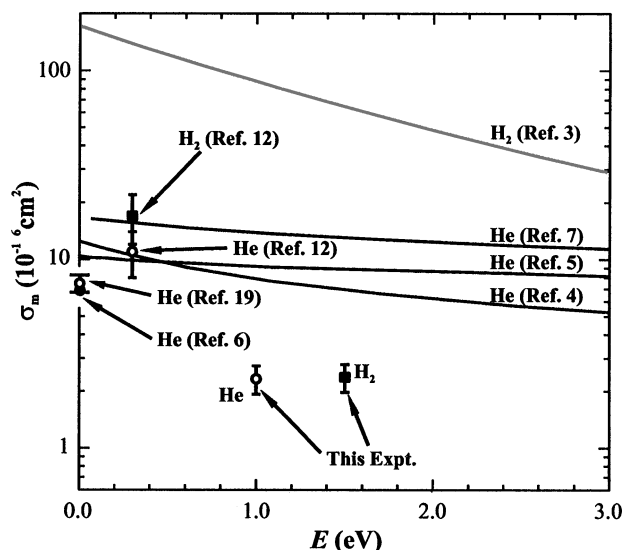


FIG. 3. Comparison of  $\text{H}_2$  and He experimental results and theoretical elastic cross sections. The molecular mass for  $\text{H}_2$  is used for  $M$  in Eq. (2).

dependence of  $\sigma_m(E)$  is strong enough. Without knowledge of this energy dependence, detailed comparison between measurements at different energies is speculative. The clear conclusion to be drawn from Fig. 3 is that complete, detailed calculations of  $\sigma_m(E)$  in this energy regime are warranted. Refinements in the DBS technique should also be able to provide more data on  $\sigma_m(E)$  for energies below 1 eV.

One important implication of these direct measurements of Ps thermalization involves the constancy of the fitted decay rate in precision measurements [13] of the o-Ps annihilation decay rate in gases. The results herein indicate that at the lowest pressures utilized in Ref. [13] the Ps might still be about 20% above room temperature at the beginning of the time window used for decay rate analysis. It should be noted that this estimate involves an extrapolation to Ps energies well below that encountered in this thermalization experiment, but the central conclusion remains that Ps was not completely thermalized in the decay rate measurement. To determine the correction on the fitted decay rate due to incomplete thermalization, it is essential to perform a separate experiment to determine how the Ps-atom collisional annihilation cross section depends on energy/temperature [20].

In conclusion, we have performed the first model-independent, direct measurements of Ps thermalizing in gases. For the seven different gases studied, reasonable fits are obtained to a simple elastic theory with constant cross sections over the Ps energy range 0.27–2.3 eV. The surprisingly linear molecular fits and the noble gas results indicate that swiftly moving Ps scatters from a single atom in the molecule, simply H for the hydrocarbons. The disparity in the theoretical cross sections demonstrates the need to fully account for both polarization and electron

exchange effects. It also compounds the difficulty of comparing theory with experiment in a case where our He and  $\text{H}_2$  results using DBS are not in agreement with those using ACAR. These cross sections appear to be significantly smaller than previously thought. The slow thermalization rates determined herein demand further investigation of incomplete thermalization in precision o-Ps decay rate measurements.

We acknowledge useful discussions with R. Conti, R. Drachman, G. W. Ford, K. Iwata, G. Laricchia, R. Lewis, R. Raymond, and J. Zorn. This research is supported by NSF Grant No. PHY 9417854 and the University of Michigan.

- [1] H. S. W. Massey and C. B. O. Mohr, Proc. Phys. Soc. London **67**, 695 (1954).
- [2] B. A. P. Page, J. Phys. B **9**, 1111 (1976); R. J. Drachman and S. K. Houston, Phys. Rev. A **14**, 894 (1976), and references therein.
- [3] M. Comi, G. M. Prosperi, and A. Zecca, Phys. Lett. **93A**, 289 (1983).
- [4] P. A. Fraser, J. Phys. B **1**, 1006 (1968).
- [5] M. I. Barker and B. H. Bransden, J. Phys. B **1**, 1109 (1968); J. Phys. B **2**, 730 (1969).
- [6] R. J. Drachman and S. K. Houston, J. Phys. B **3**, 1657 (1970).
- [7] N. K. Sarkar and A. S. Ghosh, J. Phys. B **30**, 4591 (1997).
- [8] G. Peach, (private communication); see Fig. 5 in A. J. Garner, G. Laricchia, and A. Özen, J. Phys. B **29**, 5961 (1996).
- [9] P. K. Biswas and S. K. Adhikari, Phys. Rev. Lett. (to be published).
- [10] P. G. Coleman, S. Rayner, F. M. Jacobsen, M. Charlton, and R. N. West, J. Phys. B **27**, 981 (1994).
- [11] Y. Nagashima *et al.*, Phys. Rev. A **52**, 258 (1995).
- [12] Y. Nagashima, T. Hyodo, K. Fujiwara, and A. Ichimura, The International Conference on the Physics of Electronic and Atomic Collisions, Vancouver, 1995, Abstracts of Contributed Papers (unpublished); F. Saito, N. Zafar, Y. Nagashima, and T. Hyodo, *ibid*.
- [13] C. I. Westbrook, D. W. Gidley, R. S. Conti, and A. Rich, Phys. Rev. A **40**, 5489 (1989).
- [14] W. C. Sauder, J. Res. Natl. Bur. Stand. Sect. A **72**, 91 (1968).
- [15] T. Chang, M. Xu, and X. Zeng, Phys. Lett. A **126**, 189 (1987).
- [16] D. W. Gidley, J. S. Nico, and M. Skalsey, Phys. Rev. Lett. **66**, 1302 (1991).
- [17] K. Iwata, R. G. Greaves, and C. M. Surko, Phys. Rev. A **55**, 3586 (1997); P. Van Reeth *et al.*, J. Phys. B **29**, L465 (1996).
- [18] Equation (3) disagrees with [15] by a factor of 0.678, the conversion factor from 0.5 (FWHM) to average value for energy in a Maxwell-Boltzmann distribution.
- [19] A cavity model for Ps interacting with low temperature (5–10 K) He gas is assumed in K. F. Canter *et al.*, Phys. Rev. A **12**, 375 (1975).
- [20] R. S. Vallery, R. K. Bithell, J. J. Engbrecht, D. W. Gidley, and M. Skalsey, Bull. Am. Phys. Soc. **42**, 1086 (1997).